

AD-A215 314

## Modeling the Gate I/V Characteristic of a GaAs MESFET for Volterra-Series Analysis

S. A. MAAS and A. M. CROSMUN  
Electronics Research Laboratory  
Laboratory Operations  
The Aerospace Corporation  
El Segundo, CA 90245

30 September 1989

Prepared for

SPACE SYSTEMS DIVISION  
AIR FORCE SYSTEMS COMMAND  
Los Angeles Air Force Base  
P.O. Box 92960  
Los Angeles, CA 90009-2960

APPROVED FOR PUBLIC RELEASE;  
DISTRIBUTION UNLIMITED

DTIC  
ELECTE  
NOV 24 1989  
S B D

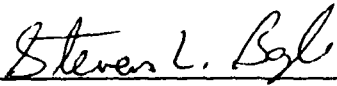
89 11 107

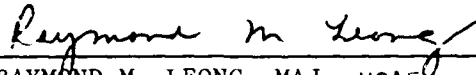
This report was submitted by The Aerospace Corporation, El Segundo, CA 90245, under Contract No. F04701-88-C-0089 with the Space Systems Division, P.O. Box 92960, Los Angeles, CA 90009-2960. It was reviewed and approved for The Aerospace Corporation by M. J. Daugherty, Director, Electronics Research Laboratory.

Lt Steve Boyle was the project officer for the Mission-Oriented Investigation and Experimentation (MOIE) Program.

This report has been reviewed by the Public Affairs Office (PAS) and is releasable to the National Technical Information Service (NTIS). At NTIS, it will be available to the general public, including foreign nationals.

This technical report has been reviewed and is approved for publication. Publication of this report does not constitute Air Force approval of the report's findings or conclusions. It is published only for the exchange and stimulation of ideas.

  
STEVE BOYLE, LT, USAF  
MOIE Project Officer  
SSD/CWHB

  
RAYMOND M. LEONG, MAJ, USAF  
MOIE Program Manager  
AFSTC/WCO OL-AB

## REPORT DOCUMENTATION PAGE

1a. REPORT SECURITY CLASSIFICATION Unclassified			1b. RESTRICTIVE MARKINGS		
2a. SECURITY CLASSIFICATION AUTHORITY			3. DISTRIBUTION / AVAILABILITY OF REPORT Approved for public release; distribution unlimited.		
2b. DECLASSIFICATION / DOWNGRADING SCHEDULE					
4. PERFORMING ORGANIZATION REPORT NUMBER(S) TR-0088(3925-02)-2			5. MONITORING ORGANIZATION REPORT NUMBER(S) SD-TR-89-72		
6a. NAME OF PERFORMING ORGANIZATION The Aerospace Corporation Laboratory Operations		6b. OFFICE SYMBOL (If applicable)	7a. NAME OF MONITORING ORGANIZATION Space Systems Division		
6c. ADDRESS (City, State, and ZIP Code) El Segundo, CA 90245			7b. ADDRESS (City, State, and ZIP Code) Los Angeles Air Force Base Los Angeles, CA 90009-2960		
8a. NAME OF FUNDING / SPONSORING ORGANIZATION		8b. OFFICE SYMBOL (If applicable)	9. PROCUREMENT INSTRUMENT IDENTIFICATION NUMBER F04701-85-C-0086-P00019		
8c. ADDRESS (City, State, and ZIP Code)			10. SOURCE OF FUNDING NUMBERS		
			PROGRAM ELEMENT NO.	PROJECT NO.	TASK NO.
					WORK UNIT ACCESSION NO.
11. TITLE (Include Security Classification) Modeling the Gate I/V Characteristic of a GaAs MESFET for Volterra-Series Analysis					
12. PERSONAL AUTHOR(S) Maas, Stephen A.; Crosmun, Andrea M.					
13a. TYPE OF REPORT		13b. TIME COVERED FROM _____ TO _____		14. DATE OF REPORT (Year, Month, Day) 1989 September 30	
				15. PAGE COUNT 17	
16. SUPPLEMENTARY NOTATION					
17. COSATI CODES			18. SUBJECT TERMS (Continue on reverse if necessary and identify by block number)		
FIELD	GROUP	SUB-GROUP	GaAs MESFETs Nonlinear circuits		
			Intermodulation distortion Volterra-series analysis		
			Nonlinear circuit analysis		
19. ABSTRACT (Continue on reverse if necessary and identify by block number)					
<p>This report shows that the Taylor-series coefficients of a FET's gate/drain I/V characteristic, which are used to model the I/V nonlinearity for Volterra-series analysis, can be derived from low-frequency rf measurements of harmonic output levels. The method circumvents many of the problems that occur when dc measurements are used to characterize this nonlinearity.</p>					
20. DISTRIBUTION / AVAILABILITY OF ABSTRACT <input checked="" type="checkbox"/> UNCLASSIFIED/UNLIMITED <input type="checkbox"/> SAME AS RPT <input type="checkbox"/> DTIC USERS			21. ABSTRACT SECURITY CLASSIFICATION Unclassified		
22a. NAME OF RESPONSIBLE INDIVIDUAL			22b. TELEPHONE (Include Area Code)		22c. OFFICE SYMBOL

# PREFACE

The authors thank R. Gowin for assistance with the fabrication of the test fixtures and M. Meyer for reviewing the manuscript.

Accession For	
NTIS GRA&I	<input checked="checked" type="checkbox"/>
DTIC TAB	<input type="checkbox"/>
Unannounced	<input type="checkbox"/>
Justification	
By	
Distribution/	
Availability Codes	
Dist	Avail and/or Special
A-1	

## CONTENTS

PREFACE.....	1
I. INTRODUCTION.....	5
II. THE MESFET MODEL.....	7
III. DESCRIPTION OF THE MEASUREMENTS.....	11
IV. EXPERIMENTAL RESULTS.....	15
REFERENCES.....	17

## FIGURES

1. Small-Signal, Nonlinear Equivalent Circuit of a GaAs MESFET.....	8
2. FET-Equivalent Circuit Valid at Frequencies in the VHF Range.....	12

## TABLE

1. Taylor-Series Coefficients for the Avantek AT10650-5.....	15
--	----

## I. INTRODUCTION

Volterra-series analysis<sup>1-3</sup> is an efficient and practical method for determining intermodulation levels in small-signal MESFET amplifiers. The Volterra series is particularly valuable when implemented in a general-purpose computer program,<sup>4</sup> because it can be used to analyze very large or complex circuits, it does not require that the circuit topology be simplified, and it is significantly more efficient than time-domain or harmonic-balance methods.

Although much research has been directed at developing large-signal FET models for use with harmonic-balance analysis, very little work has been done to model GaAs MESFETs for Volterra-series analysis. Modeling GaAs MESFETS presents a number of subtle problems that occasionally have been noted by other authors (e.g. Refs. 5, 6); one of the most serious of these problems is the difficulty of modeling the FET's "nonlinear transconductance," or more precisely its nonlinear incremental gate/drain I/V characteristic. This report describes a method for determining the parameters of this characteristic by means of simple, low-frequency rf measurements.

## II. THE MESFET MODEL

Figure 1 shows a small-signal nonlinear model of a MESFET. This model consists of a modified conventional small-signal linear model, in which three elements -- the gate/source capacitance  $C_{gs}$ , the drain/source resistance  $R_{ds}$ , and the drain current  $i_d(v_g)$  -- are nonlinear. Although  $C_{gs}$  and  $R_{ds}$  are significant sources of intermodulation in small-signal FETs, in most cases the dominant nonlinearity is that of  $i_d(v_g)$ .

The nonlinear resistive elements are characterized by Taylor-series expansions of their I/V characteristics in the vicinity of the dc bias point. Thus, the nonlinearity  $i_d(v_g)$  is

$$i_d = \left. \frac{dI_d(v_g)}{dv_g} \right|_{v_g=v_{g,0}} v_g + \frac{1}{2} \left. \frac{d^2 I_d(v_g)}{dv_g^2} \right|_{v_g=v_{g,0}} v_g^2 + \frac{1}{6} \left. \frac{d^3 I_d(v_g)}{dv_g^3} \right|_{v_g=v_{g,0}} v_g^3 + \dots \quad (1)$$

where  $I_d(v_g)$  is the large-signal gate/drain characteristic and  $i_d$  and  $v_g$  are, respectively, the incremental (rf) drain and gate currents and voltages, i.e., the current and voltage deviations from the bias point  $I_d(v_{g,0})$ . Then  $i_d$  is expressed as

$$i_d = a_1 v_g + a_2 v_g^2 + a_3 v_g^3 + \dots \quad (2)$$

The traditional method of determining the series coefficients  $a_n$  is to measure the I/V characteristic at a fixed drain-bias voltage and to perform a least-squares fit of  $i_d(v_g)$  to a polynomial of the desired degree. Although this process is usually adequate for determining  $a_1$  (which is equivalent to the linear transconductance), it is often unsatisfactory for determining the higher-order coefficients: because of the ill-conditioned nature of the normal equation, the values of  $a_n$  determined in this manner are very sensitive to measurement inaccuracy, round-off errors, and the selection of data points.

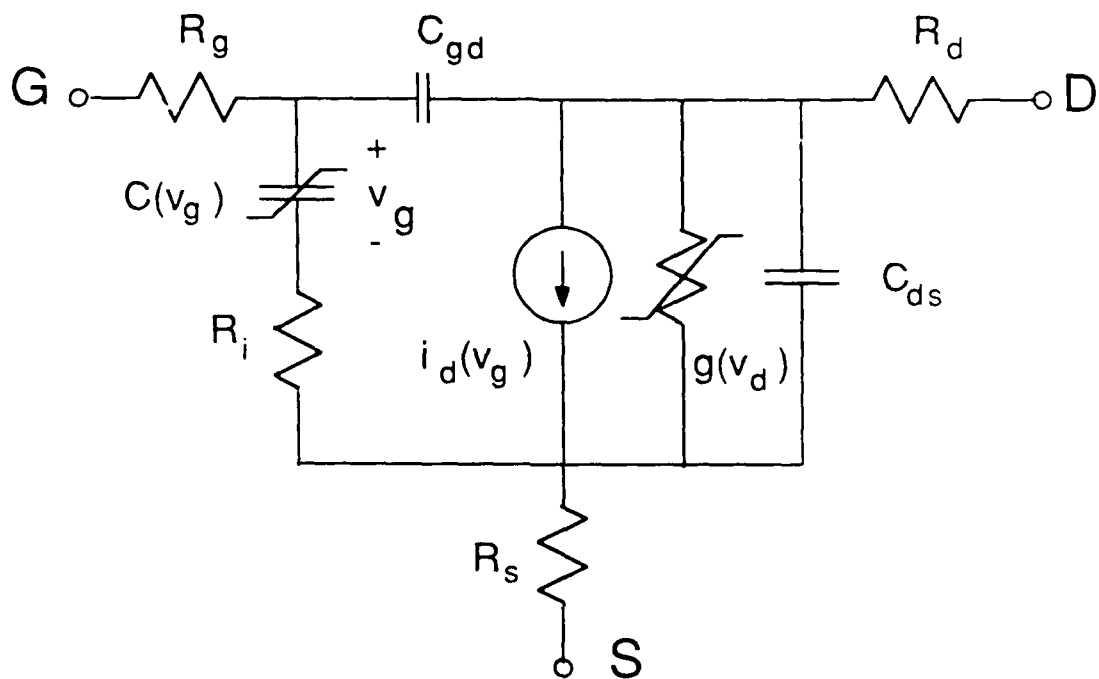


Fig. 1. Small-Signal, Nonlinear Equivalent Circuit of a GaAs MESFET



Differentiating the measured data directly is often adequate for determining  $a_1$  and sometimes  $a_2$ ; however, differentiation exacerbates the effects of round-off errors and thus makes the higher derivatives unreliable.

A more fundamental problem is related to traps in the FET's channel; these introduce long time constants into  $i_d(v_g)$  and cause differences between the dc and rf I/V characteristics. Trapping effects are often not evident in  $a_1$  or  $a_2$ , but derivatives of higher order are very sensitive to them. This is particularly the case when automated equipment is used to measure  $I_d(V_g)$ ; differences in stepping speed and dwell time at each data point affect the coefficients' values strongly.

An effective way of circumventing these problems is to derive the series coefficients from rf measurements instead of dc. The rf measurements are made at a frequency in the VHF range, at which both trapping effects and the FET's reactive parasitics are negligible. Under these conditions the levels of the harmonic output components are functions of only the input power, the FET's source resistance, and the series coefficients. It is a simple matter to measure the harmonic levels and to derive the coefficients from them.

### III. DESCRIPTION OF THE MEASUREMENTS

When the rf frequency is very low, the equivalent circuit of Figure 1 can be simplified to form the circuit shown in Fig. 2. In Fig. 2 the FET is driven by an rf source at a frequency of approximately 50 MHz, and the drain is terminated in a load resistance  $R_L$ , where  $R_L \ll R_{ds}$ .  $R_L$  is a shunting resistor that reduces the current in  $R_{ds}$  to the point where its effects are negligible; one should make  $R_L$  as small as possible while still allowing harmonic output components to be observable on a spectrum analyzer. Because the series coefficients are derived from the relative levels of the harmonics, and not their absolute powers, the value of  $R_L$  does not affect the accuracy of the measurement.

Using the method of nonlinear currents,<sup>2,3</sup> one can show that the first three harmonics of the drain current,  $I_{1-3}$ , are

$$I_1 = \frac{a_1 V_{gs}}{1 + a_1 R_s} \quad (3)$$

$$I_2 = \frac{a_2 (1 - a_1 R_s) V_{gs}^2}{2(1 + a_1 R_s)^2} \quad (4)$$

$$I_3 = \frac{(a_3 - 2a_2^2 R_s)(1 - a_1 R_s) V_{gs}^3}{4(1 + a_1 R_s)^3} \quad (5)$$

$V_{gs}$  is the magnitude of  $v_{gs}(t)$ ; i.e.,

$$v_{gs}(t) = V_{gs} \cos(\omega t) \quad (6)$$

and the available power  $P_a$  of the source is

$$P_a = \frac{V_{gs}^2}{8 R_{in}} \quad (7)$$

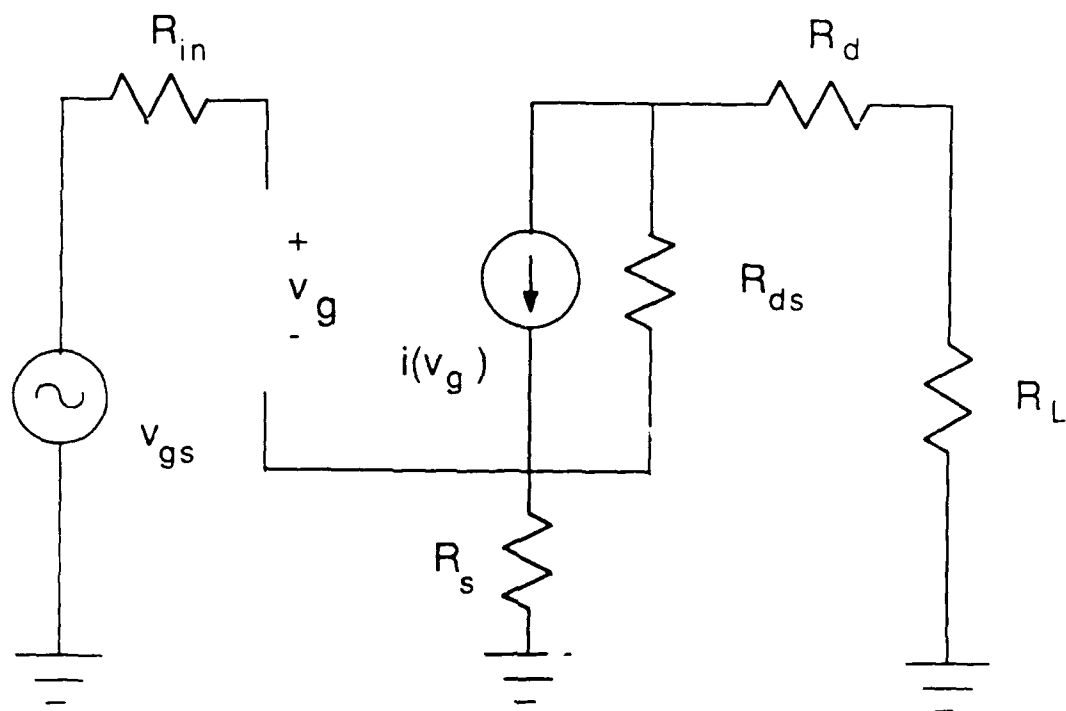


Fig. 2. FET-Equivalent Circuit Valid at Frequencies in the VHF Range.  $R_L$  is the output-shunting resistor used to minimize harmonic generation in  $R_{ds}$ .

where  $R_{in}$  is the source resistance.

Substituting Eq. (7) into Eqs. (3) and (4), dividing Eq. (4) by Eq. (3), and squaring the result gives the ratio of second-harmonic output power to fundamental output power,  $IMR_2$ :

$$IMR_2 = \frac{2 a_2^2 R_{in} (1 - a_1 R_2)^2 P_a}{a_1^2 (1 + a_1 R_s)^2} \quad (8)$$

A similar process gives the ratio of third-harmonic output power to fundamental output power,  $IMR_3$ :

$$IMR_3 = \left[ \frac{2(a_3 - 2a_2^2 R_s)(1 - a_1 R_s) R_{in}}{a_1 (1 + a_1 R_s)^2} \right]^2 P_a^2 \quad (9)$$

When the FET is biased and excited by a low-frequency rf source, the values of  $a_n$  can be found by measuring the harmonic output power and solving Eqs. (7) through (9). The process is as follows:

1.  $a_1$  is determined in the conventional manner, i.e., by dc or rf measurements.
2.  $IMR_2$  is measured by means of a spectrum analyzer, and Eq. (8) is solved to determine  $a_2$ .
3.  $IMR_3$  is measured similarly, and Eq. (9) is solved to determine  $a_3$ .

Equation (8) does not indicate whether  $a_2$  is positive or negative. However, because a MESFET's transconductance invariably rises with  $v_g$ ,  $a_2$  is invariably positive (this is generally not the case in HEMTs, but even then the regions of positive and negative  $a_2$  are clear from the transconductance curve). Because of the squared term in brackets, two values of  $a_3$  satisfy Eq. (9). One can determine the correct root by measuring a few values of  $a_2$  at nearby bias points and picking the value of  $a_3$  that most closely matches  $a_3 = 0.33 da_2/dv_g$ . Usually the two values of  $a_3$  have different signs; then, to select the correct value of  $a_3$ , one need determine only whether  $a_2$  rises or falls with  $v_g$ .

#### IV. EXPERIMENTAL RESULTS

This method was used to determine the incremental gate I/V characteristic of a packaged Avantek AT10650-5 MESFET biased at a drain voltage of 3 V and drain current of 20 mA. The FET's transconductance was measured at dc, and its small-signal equivalent circuit (including the package parasitics) was determined by adjusting its circuit-element values until good agreement between calculated and measured S parameters was obtained. The FET was then installed in a low-frequency test fixture having a shunting resistance  $R_L$  of 5 ohms. The input power  $P_a$  was -11 dBm at a frequency of 50 MHz.

The  $a_n$  coefficients were determined at 19, 20, and 21 mA, and the values in Table 1 were obtained. The coefficient  $a_2$  was found to decrease with  $I_d$ , and the two roots of Eq. (9) had different signs; therefore the negative value of  $a_3$  is the correct one.

Table 1. Taylor-Series Coefficients  
for the Avantek AT10650-5

$I_d$	$a_1$	$a_2$	$a_3$
0.019	0.041	0.0188	-0.0148
0.020	0.041	0.0171	-0.0145
0.021	0.041	0.0158	-0.0128

The FET's gate/source capacitance was modeled as an ideal Schottky-barrier junction capacitance, and the nonlinear drain/source resistance was derived from low-frequency Y parameters measured at a variety of bias voltages. When the source and load terminations were 50 ohms, the program described in Ref. 4 predicted the FET's third-order intermodulation intercept point to be 20.8 dBm at 10 GHz. This result

agrees well with the measured value of the intercept point, which was 22.4 dBm. When the output port was conjugate matched, the calculated intercept point was 24.1 dBm, compared to a measured value of 23.0 dBm. Other tests have shown equal or superior agreement. These results imply that the intermodulation levels in small-signal amplifiers can be predicted within 2 to 3 dB. We believe that the major factor limiting accuracy is the linear part of the FET's equivalent-circuit model, especially the part that models the package. Thus, even better accuracy could be obtained with chip or MMIC circuits.

#### REFERENCES

1. D. D. Weiner and J. F. Spina, Sinusoidal Analysis and Modeling of Weakly Nonlinear Circuits (Van Nostrand, New York, 1980).
2. J. J. Bussgang, L. Ehrman, and J. W. Graham, "Analysis of Nonlinear Systems with Multiple Inputs," Proc. IEEE 62 [8], 1088-1119 (August 1974).
3. S. A. Maas, Nonlinear Microwave Circuits (Artech House, Norwood, Mass., 1988).
4. S. A. Maas, "A General-Purpose Computer Program for the Volterra-Series Analysis of Nonlinear Microwave Circuits," IEEE MTT-S International Microwave Symposium Digest (1988), p. 311.
5. R. A. Minasian, "Intermodulation Distortion Analysis of MESFET Amplifiers Using the Volterra Series Representation," IEEE Trans. Microwave Theory Tech. MTT-28 [1], 1 (January 1980).
6. C. L. Law and C. S. Aitchison, "Prediction of Wide-Band Power Performance of MESFET Distributed Amplifiers Using the Volterra Series Representation," IEEE Trans. Microwave Theory Tech. MTT-34 [12], 1308 (December 1986).

## LABORATORY OPERATIONS

The Aerospace Corporation functions as an "architect-engineer" for national security projects, specializing in advanced military space systems. Providing research support, the corporation's Laboratory Operations conducts experimental and theoretical investigations that focus on the application of scientific and technical advances to such systems. Vital to the success of these investigations is the technical staff's wide-ranging expertise and its ability to stay current with new developments. This expertise is enhanced by a research program aimed at dealing with the many problems associated with rapidly evolving space systems. Contributing their capabilities to the research effort are these individual laboratories:

Aerophysics Laboratory: Launch vehicle and reentry fluid mechanics, heat transfer and flight dynamics; chemical and electric propulsion, propellant chemistry, chemical dynamics, environmental chemistry, trace detection; spacecraft structural mechanics, contamination, thermal and structural control; high temperature thermomechanics, gas kinetics and radiation; cw and pulsed chemical and excimer laser development including chemical kinetics, spectroscopy, optical resonators, beam control, atmospheric propagation, laser effects and countermeasures.

Chemistry and Physics Laboratory: Atmospheric chemical reactions, atmospheric optics, light scattering, state-specific chemical reactions and radiative signatures of missile plumes, sensor out-of-field-of-view rejection, applied laser spectroscopy, laser chemistry, laser optoelectronics, solar cell physics, battery electrochemistry, space vacuum and radiation effects on materials, lubrication and surface phenomena, thermionic emission, photo-sensitive materials and detectors, atomic frequency standards, and environmental chemistry.

Computer Science Laboratory: Program verification, program translation, performance-sensitive system design, distributed architectures for spaceborne computers, fault-tolerant computer systems, artificial intelligence, micro-electronics applications, communication protocols, and computer security.

Electronics Research Laboratory: Microelectronics, solid-state device physics, compound semiconductors, radiation hardening; electro-optics, quantum electronics, solid-state lasers, optical propagation and communications; microwave semiconductor devices, microwave/millimeter wave measurements, diagnostics and radiometry, microwave/millimeter wave thermionic devices; atomic time and frequency standards; antennas, rf systems, electromagnetic propagation phenomena, space communication systems.

Materials Sciences Laboratory: Development of new materials: metals, alloys, ceramics, polymers and their composites, and new forms of carbon; non-destructive evaluation, component failure analysis and reliability; fracture mechanics and stress corrosion; analysis and evaluation of materials at cryogenic and elevated temperatures as well as in space and enemy-induced environments.

Space Sciences Laboratory: Magnetospheric, auroral and cosmic ray physics, wave-particle interactions, magnetospheric plasma waves; atmospheric and ionospheric physics, density and composition of the upper atmosphere, remote sensing using atmospheric radiation; solar physics, infrared astronomy, infrared signature analysis; effects of solar activity, magnetic storms and nuclear explosions on the earth's atmosphere, ionosphere and magnetosphere; effects of electromagnetic and particulate radiations on space systems; space instrumentation.